

Oxidation Behavior and Decomposition Kinetics of Mixed-Waste Biomass Material

Po-Heng Lin,^{a,b} Chun-Han Ko,^{a,*} Fang-Chih Chang,^{c,*} San-Hsien Tu,^b and Cheng-Jung Lin^b

In Taiwan, approximately 379,000 automobiles and 588,000 motorcycles were recycled in 2019. Rigid polyurethane foam is one of the principal components of auto shredder residue. The amount of rigid polyurethane foam from the recycling of waste vehicles is 8,000 to 10,000 tons/year. In this study, waste *Cryptomeria* wood was mixed with waste rigid polyurethane foam to form derived fuels. The oxidation behaviors of the wood mixed with waste rigid polyurethane foam-derived fuels were investigated. The characteristics of the derived fuel made from wood mixed with waste rigid polyurethane foam showed that the ash content was less than 2.5% and its calorific value reached 21.9 MJ/kg. According to the Friedman equation, the activation energies of the wood mixed with 5%, 15%, and 30% of waste rigid polyurethane foam pellets were 212, 220, and 188 kJ/mol, respectively. The thermal conversion efficiencies of the wood mixed with 5%, 15%, and 30% of waste rigid polyurethane foam pellets were 30.2% to 48.1% by a water boiling test. The results showed that waste *Cryptomeria* mixed with waste rigid polyurethane foam-derived fuels is suitable for use as an alternative renewable energy fuel.

DOI: 10.15376/biores.18.1.778-791

Keywords: Waste-derived fuels; Recycling; Waste rigid polyurethane foam; Activation energy; Biomass

Contact information: a: School of Forestry and Resource Conservation National Taiwan University, Taipei 10617, Taiwan; b: Taiwan Forestry Research Institute, Taipei 100, Taiwan; c: The Experimental Forest, College of Bio-Resources and Agriculture, National Taiwan University, Nantou 55750, Taiwan;

* Corresponding authors: chunhank@ntu.edu.tw; d90541003@ntu.edu.tw

INTRODUCTION

Since the Industrial Revolution, human beings have adopted a linear and non-recyclable way of producing and consuming resources. At the same time, rapid globalization and intensified consumerism have driven the demand for energy and generated plastic and related wastes. In 2020, Taiwan generated approximately 1,994,000 tons of plastic waste, of which 6.14% was recycled, 39.05% was used for energy recovery, and the rest was placed in landfills, (Taiwan EPA, 2020).

Foam polyurethane is one type of plastic waste. It is synthesized from major raw materials such as polyols and polyisocyanates, and auxiliary raw materials such as chain extenders, bridging agents, modifiers, or catalysts (Gama *et al.* 2018). Different processing methods for foam polyurethane can produce a variety of products, with good physical and chemical properties, good wear resistance, high flexibility, high elongation, ease of processing, and excellent elasticity. Products with different uses are widely used in plastics, rubber, fibers, coatings, adhesives, and other fields (Deng *et al.* 2021).

Polyurethane is mainly disposed of in landfills, but after secondary pollution and non-corrosion problems have arisen in recent years, this has completely changed to incineration treatment (Datta and Włoch 2017). However, incineration plants are faced with problems such as extension or transformation (larger storage space for wood waste and foam polyurethane), and recycling must take into account the technical maturity and lightweight characteristic of the foam and its large volume, which leads to high transportation costs to treatment plants (Park *et al.* 2018). Treatment methods have resulted in serious environmental damage and low energy efficiency (Singh *et al.* 2016).

Biomass is an important and abundant renewable resource. Plants of agriculture and forestry absorb the energy of sunlight during their growth and produce glucose through photosynthesis by combining CO₂ and H₂O. As biomass burns, the carbon trapped inside is released into the atmosphere, from where it can be recycled again in a photosynthetic process. Therefore, biomass energy has the characteristic of carbon neutrality when calculating zero output of carbon dioxide from biomass fuel combustion. Using biomass fuel as the main alternative energy can help reduce the consumption of fossil fuels, and it also reduces impacts of a strong greenhouse effect on the global environment, which is beneficial to the sustainable development of the environment (Bilgili *et al.* 2017). However, biomass has high water contents, low calorific values, low energy densities, and complex compositions. Moreover, biomass faces the dilemma of seasonal supplies, scattered distributions, and costs derived from high-cost transportation and storage. These make the conversion of thermal energy into energy quite challenging (REN21 2018).

Among the various densification options that increase the bulk density and decrease the volume, pelleting and briquetting are the most common methods of solid biofuel production (Younis *et al.* 2018). Both pellets and briquettes have different production technologies and market demands, which are also helpful for back-end storage and transportation. Biomass can be directly combined with plastics and other solid fuels to generate refuse-derived fuels (RDFs), including lignocellulosic biomass (wood, grass, energy crops, and agricultural residues) with waste polymers (plastics and waste tires) (Zhang *et al.* 2016), red oak with high-density polyethylene (Xue *et al.* 2015), cedar wood, sunflower stalks, and Asian knotweed (*Fallopia japonica*) with low-density polyethylene (LDPE; Yang *et al.* 2016), *etc.* Plastic wastes all have characteristics of high calorific values and can be converted into solid biomass fuel to increase the unit energy density (Vanapalli *et al.* 2021).

In order to achieve the UN Sustainable Development Indicators and Net Zero by 2050, the importance of green renewable energy and the recycling of waste are increasing due to the natural abundance and sustainability of green renewable materials. Waste *Cryptomeria* wood was mixed with waste rigid polyurethane foam to form the waste derived fuels. Residual materials of cedar (*Cryptomeria*) collected from local lumber yards were supplemented with different weight ratios of recycled rigid foam from automobiles and uniformly mixed, and the RDF process was carried out in a ring die granulator. The heat loss was analyzed by thermogravimetric analysis (TGA). A thermodynamic model was constructed using Friedman methods at different heating rates, and combustion-related parameters were calculated. The heat conversion efficiencies, exhaust gas compositions, and suspended particulate concentrations of boiler combustion were also evaluated to establish multi-target utilization of local independent biomass energy resources and their sustainable use.

EXPERIMENTAL

Materials

The samples used in this study consisted of waste wood and discarded rigid polyurethane (PU) foam, and after being crushed, the components were uniformly mixed and granulated. Wooden material was obtained from a local sawmill, while the PU was previously used in the automotive industry. The waste wood was crushed by SY-101 Small Fast Speed Crusher (Shiang Young Machinery, Taiwan). The discarded rigid polyurethane (PU) foam was crushed by RT-08 Pulverizing Machine (Rong Tsong Iron Work, Taiwan). Samples were prepared with the following percentages: 100% wooden material (wood), wood mixed with 5% PU (WMP5), wood mixed with 15% PU (WMP15), wood mixed with 30% PU (WMP30), and PU.



Fig. 1. Sample of wooden material (wood), wood mixed with PU, and rigid PU foam

Waste Refuse-Derived Fuel (RDF)

The waste wood and discarded rigid PU foam were crushed into granules and sieved (<6 mm), and then PU was mixed together with the wood powder at weight ratios of 5%, 15%, and 30% of rigid PU foam added to wood biomass. The mixed biomass was extruded into waste refuse-derived pellets (with a diameter of 6 mm and length of 40 mm).

Methods

The raw materials were analyzed to obtain their basic properties and compositions, including a wood chemical composition analysis, a proximate analysis, and an elemental analysis. Then, samples were analyzed with an oxygen bomb calorimeter and a thermal gravimetric (TG) analyzer to respectively determine their energy contents and thermal behaviors. The RDF fuels were combusted in a custom-made Philips furnace. Flue gas was analyzed to understand dynamic changes in the gas composition during the RDF fuel process, and the concentration of particulate matter with an aerodynamic diameter of < 2.5 μm (PM_{2.5}) of the exhaust gas was simultaneously monitored. The thermal conversion efficiency was also calculated by a boiling water test.

Wood Characteristic Analysis

The chemical composition of wood can generally be divided into cellulose, hemicellulose, lignin, extractives, and ash. Before chemicals react with cellulose, hemicellulose, and lignin, the extractives need to be isolated by alcohol-benzene extraction. Then, cellulose, hemicellulose, and lignin can be separated. Ash is the inorganic substance in wood and can be segregated by burning. The methods below are based on CNS 452 (2013), CNS 4713 (2005), CNS 3084 (2004), CNS 3085 (2004), CNS 14907 (2005), and CNS 12108 (1987). A proximate analysis can divide compounds into moisture, volatiles, fixed carbon, and ash (CNS 10821 (1984), CNS 10822 (1984), CNS 10823 (1984), and CNS 10824 (1984)). For more-precise determination, the materials were sent to be tested

with an elemental analyzer. It provided the compositions of C, H, N, S, and O, and can be a reference for the heating value. The instrument was an Elementar vario EL CUBE, and the measurement was NIEA R409.21c (2004). The dry-basis heating value analysis was based on NIEA R214.01c (2005), and the method of the waste calorific value was based on an adiabatic bomb calorimeter, at the Environmental Analysis Laboratory.

Kinetic Analysis

The activation energy was calculated using methods developed by Friedman (1964), Ozawa (1965 and 1971), and Kissinger (1956 and 1957). Owing to the complicated oxidation of the biomass materials, it was impossible to accurately predict the reaction mechanism. However, the overall oxidation reaction mechanism was proposed by Sadhukhan *et al.* (2011) as the Friedman method, as follows,

$$\ln \left(\frac{d\alpha}{dt} / e^{-\frac{E_a}{RT}} \right) = \ln A + n \ln(1 - \alpha) \quad (1)$$

where α is the pyrolytic degradation conversion degree, A is the pre-exponential factor (min^{-1}), E_a is the activation energy ($\text{kJ}\cdot\text{mol}^{-1}$), R is the gas constant ($8.314 \text{ J}\cdot\text{K}^{-1}\cdot\text{mol}^{-1}$), T is the absolute temperature, and n is the order of the reaction.

Combustion Parameters

Combustion parameters can be used to evaluate the combustion characteristics of a sample, and include the reactivity, ignition temperature, ember temperature, *etc.* Parameter calculations for biomass samples under oxidative conditions were determined according to the method used by Okoroigwe *et al.* (2016). Reactivity (R_M) is a measure of the reactivity of the sample in the decomposition stage using the height of the DTG curve, as follows,

$$R_M = 100 \Sigma (R_{DTG_{\max}} / T_{DTG_{\max}}) \quad (2)$$

where $R_{DTG_{\max}}$ is the maximum weight loss rate and $T_{DTG_{\max}}$ is the corresponding peak temperature.

The ignition temperature (T_i) is the temperature at which the biomass sample begins to undergo major decomposition. The ember temperature (T_b) is defined as the temperature at which there is no significant weight loss in the TG or DTG curves. The ignition index (D_i) and combustion index (S) are calculated using the following two equations,

$$D_i = \frac{R_{\max}}{t_m t_i} \text{ and} \quad (3)$$

$$S = \frac{R_{\max} R_a}{T_i^2 T_b} \quad (4)$$

where R_{\max} is the maximum combustion rate ($\% \cdot \text{C}^{-1} \cdot \text{s}^{-1}$) being the peak point on the DTG curve in the combustion zone, t_m is the time (s) corresponding to the maximum combustion rate, t_i is the time (s) corresponding to the ignition temperature, R_a is the average mass loss rate under oxidative conditions ($\% \cdot \text{s}^{-1}$), T_i is the ignition temperature ($^{\circ}\text{C}$), and T_b is the burn-out temperature ($^{\circ}\text{C}$).

Experimental Rig

The furnace used in the experiment was a forced-air Philips furnace produced by a local manufacturer. The body of the stove was made of white iron. The diameter of the furnace body was 15 cm and its height was 60 cm. The appearance was cylindrical, and

there was a forced near-air fan at the bottom, which actively took air into the furnace body and led to the upper end of the furnace body along the inner and outer furnace body channels for combustion. Due to the low inlet temperature and high density, the generated gas was forced to prolong the combustion time, resulting in an improvement in the quality of the exhaust flue gas. The feeding port was on the upper side of the furnace body and had a gravitational movable door to keep the furnace body closed during the process of no feeding, so as to avoid affecting the combustion process. During the combustion process, the flue gas temperature at the furnace outlet was monitored synchronously in real time, and concentrations of CO, O₂, NO_x, SO₂, and PM_{2.5} in the flue gas were measured using the following instruments.



Fig. 2. Diagram of the custom-made boiler

The flue gas analyzer used was a 2800P Flue Gas Analyzer (IMR Environmental Equipment, St. Petersburg, FL, USA). The IMR 2800P is a portable Flue Gas Analyzer for industrial applications. The flue gas analyzer uses electrochemical methods to measure the O₂ (0%-21% range), CO (0-4000 ppm range), NO (0-2000 ppm range), NO₂ (0-100 ppm range), and SO₂ concentrations (range 0-4000 ppm). The PM_{2.5} detector used was a DustTrak II Aerosol Monitor 8530 (TSI, Shoreview, MN, USA). The DRX Aerosol Monitor can measure both the mass and size fraction at the same time and provides a gravimetric sample. It is suitable for indoor and outdoor applications, industrial and occupational hygiene, baseline screening, remote monitoring, and research studies. The DustTrak II Aerosol Monitor measures aerosol contaminants such as dust, smoke, fumes, and mists.

Water Boiling Test

After the fuel was ignited, a pot with 5 L of water and a lid was placed on the stove to begin the test according to Chen *et al.* (2016). When the water temperature reached the boiling point, the lid was removed. The fuel remaining in the furnace was left to burn. When the water temperature dropped to 5 °C below the boiling point, the test ended, and the amount by which the water was reduced was calculated by converting the heat of evaporation under 1 atm of water to calculate the boiler efficiency.

RESULTS AND DISCUSSION

As shown in Table 1, the main chemical components of the remaining materials of *Cryptomeria fortunei*, such as total cellulose and hemicellulose, were similar to previous results by Chen *et al.* (2014). The results obtained from the chemical analysis were as follows: 32.33% lignin, 41.15% cellulose, 19.56% hemicellulose, 0.73% ash, and 6.43% other components (extracts). The lignin value was close to 30.66% to 33.78% in a range for cedar in previous research. The percentages of cellulose obtained also fell within literature values (38.67% to 43.80%), while hemicellulose values were lower than values reported in the literature of 20.77% to 23.16%. Those researchers found that the extract value was 3.47% to 7.80%, and the results obtained here were within this range, while the ash value was higher than 0.31% to 0.57% of previous studies (Lu *et al.* 2013; Rabemanolontsoa and Saka 2013; Lin *et al.* 2022).

Table 1. Chemical Analysis of Wood

Holocellulose (%)	α -Cellulose (%)	Lignin (%)	Extractives and Others (%)	Ash (%)
60.71	41.15	32.33	6.43	0.73

Table 2. Three-Component, Elemental Analysis, and Calorific Value (Dry-Based) of the Waste and Wood

Property	Wood and Percent Waste				Waste
	0%	5%	15%	30%	
Moisture (%)	6.21	5.26	4.85	4.06	1.02
Ash (%)	0.73	1.30	1.45	1.73	2.05
Combustible portion (%)	93.06	93.44	93.7	94.21	96.93
C (%)	47.87	48.57	50.46	56.64	63.71
H (%)	6.59	6.72	6.68	6.70	6.84
O (%)	43.13	38.50	37.04	29.76	22.09
N (%)	0.10	1.39	1.92	4.05	7.07
S (%)	N.D.	N.D.	N.D.	N.D.	N.D.
Calorific value (MJ·kg ⁻¹)	18.54	19.15	20.57	21.91	24.12

The TG and DTG of the samples are shown in Fig. 3. These results indicated that the primary oxidative decomposition of all samples followed a similar oxidative degradation stage, and the proportion of the secondary oxidative stage increased as the proportion of the reference PU material increased.

In these experiments, the TG and DTG curves of the percentage of weight degradation at elevated temperatures are presented. The degradation trends of WP, WMP5, WMP15, and WMP30 were similar. However, the PU part had a different TGA loss pattern than the previous samples. The overall reactions all exhibited three main stages of biomass combustion, namely dehydration and the two main thermal oxidation stages. The first-stage sample underwent a morphological change and the system provided thermal energy to evaporate the water.

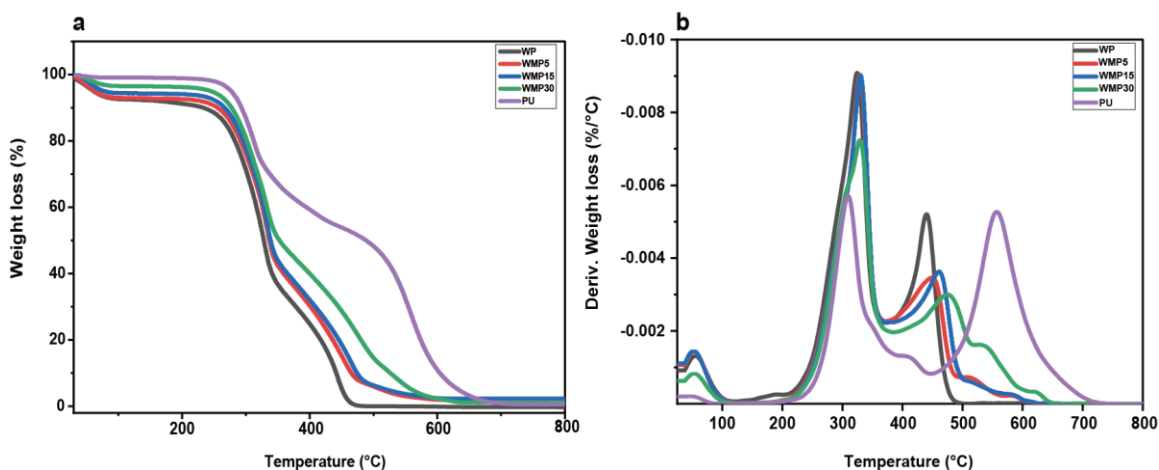


Fig. 3. (a) Thermogravimetric (TG) and (b) DTG curves for different pellets at a heating rate of $10\text{ }^{\circ}\text{C}\cdot\text{min}^{-1}$

The second stage of biomass combustion occurred in an aerobic environment and continued to receive heat from the system for primary mass loss thermal oxidation, which is usually the most intense at this stage. In the third stage, as the system temperature increased, the deep volatile components of the biomass and perhaps also of the PU contributed. The second and final step was the decomposition phase. During this period, the sample achieved complete combustion in the presence of oxygen. The sample was decomposed into volatiles and ash (Garrido and Font 2015).

These results indicated that the thermal decomposition of all samples could be understood by analyzing the thermal species loss and thermal species differential curve. Structural decomposition of the sample passed through three similar stages. The first stage was the dehydration stage from 20 to 200 °C, this stage was mainly due to the weight loss of moisture and some volatile substances in the sample. The second stage of the active combustion stage was from 200 to 550 °C, which was the volatile decomposition (oxidation) stage. The cellulose and lignin were broken down in the second stage. With the exception of PU, all samples experienced the greatest quality loss in this stage, although their differences caused quality losses at different temperatures. The third stage of the passive active combustion stage was from 550 to 800 °C, and the weight losses of the samples were all $< 2.0\%$, except for PU. The final residual content was 0.73% to 2.05%, which increased with increments of the PU content.

The main thermal decomposition of the sample followed two-stage structural decomposition. The first stage consisted of a temperature rise from 160 to 380 °C, which was the region where cellulose and hemicellulose decomposed (Luo *et al.* 2018). All samples, except for PU, experienced the greatest mass loss at this stage, although the mass loss at this stage differed at different temperatures due to the different PU reference compositions. In the second stage, decomposition ranges of samples without PU and samples with smaller proportions of PU, such as WP, WP5, and WP15, were 380 to 610 °C, but that of the WP30 sample was 380 to 640 °C and that for PU was 380 to 730 °C. The extent of regional decomposition also increased with an increasing PU content (Branca *et al.* 2003).

The reactivities of samples in the oxidation and carbonization combustion stages are shown in Table 3. The reactivity index, R_M , is an index to measure the decomposition speed of structural components, which was measured by the peak value of the DTG curve.

Results show that during the re-burning process, the reactivity of PU was the lowest, while the reactivity of the sample decreased with an increase of the proportion of PU added. T_{peak} and the maximum weight loss rate also exhibited a similar situation. As the proportion of PU addition increased, the sample T_{peak} and maximum weight loss rate also decreased.

The ignition (D_i) and combustion indices (S) of the sample are shown in Table 3. The sample without added wood showed the lowest ignition temperature, T_i , 282.6 °C, while WMP5 showed the highest T_i of 291.1 °C, and the ignition index equaled 7.84×10^7 %·°C⁻¹·s⁻². All of this could be attributed to the relative reactivity. The burn-out temperature is applied to represent the combustion characteristics of a fuel. It is defined as the temperature at which the rate of weight loss continues to drop to <1%·min⁻¹. At this temperature, the decomposition of the sample can be considered to be almost complete, and there is no further significant mass loss in the form of volatiles. Table 3 lists the burn-out temperatures, T_b , of the biomass samples we examined. Generally, a low burn-out degree indicates that a sample easily burned out; the lower the burn-out temperature, the easier the fuel burns. Among all the samples, wood exhibited the lowest burn-out temperature (of 460.7 °C), which meant that it burned more easily than the other samples, while PU exhibited the highest burn-out temperature (of 671.2 °C), and it increased with an increasing PU content. The burn-out temperature also increased simultaneously.

Table 3. Characteristic Combustion Parameters of the Biomass Blends at a Heating Rate of 10 °C/min

Sample	Mean reactivity $R_M \cdot 10^3 (\%/s^\circ\text{C})$	T_i (°C)	T_b (°C)	t_m (s)	t_i (s)	$D \cdot 10^8$	$S \cdot 10^{10}$
Wood	0.669	282.61	460.667	1735	1546	7.84	2.75
WMP5	0.521	291.06	577.50	1809	1596	5.90	1.22
WMP15	0.512	290.77	581.33	1806	1595	5.80	1.18
WMP30	0.394	284.91	619.17	1806	1560	4.55	0.83
PU	0.300	281.21	692.17	1709	1537	3.54	0.49

The activation energy is the threshold energy of any sample undergoing a chemical reaction, which is usually overcome before the reaction proceeds. The activation energy is the minimum energy required to initiate the decomposition reaction. In the kinetic analysis, $\ln(\beta d\alpha/dT)$ vs. $1/T$ obtained by the Friedman equation was linear (as shown in Fig. 4). In this study, the Friedman method was used to investigate the thermodynamics and calculate its activation energy and other kinetic parameters. This method is based on the same conversion rate and the remaining reactants having a fixed chemical composition. The TG curve of the same sample is scanned at different heating rates. Under the same conversion rate, the relationship between $\ln(d\alpha/dt)$ and $1/T$ is plotted to obtain the kinetic parameters. This method uses iso-conversional methods to deduce that the model had a highly linear relationship, and the R^2 of all samples exceeded 0.9716, which was highly correlated with the combustion process, so more-accurate E_a values could be obtained (Huang *et al.* 2018). Average E_a values of the WP, WMP5, WMP15, WMP30, and PU samples obtained by this method were 188.50, 175.66, 165.38, 152.55, and 124.61 kJ·mol⁻¹, respectively. An R^2 value close to 1 indicates that the kinetic model used for such samples is the best description of the oxidation/combustion process. Compared to the previous literature, the E_a calculated

by the Friedman method in the combustion process of cedar (WP) was slightly lower than that of African border tree wood ($231.3 \text{ kJ}\cdot\text{mol}^{-1}$) and higher than that of African bush mango wood ($131.5 \text{ kJ}\cdot\text{mol}^{-1}$) (Okoroigwe *et al.* 2016).

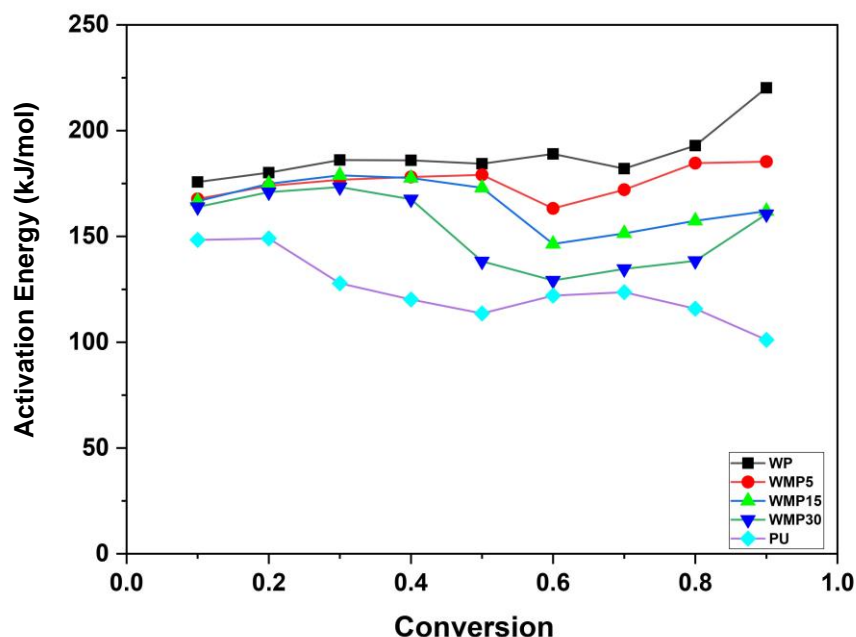


Fig. 4. Activation energies of waste refuse-derived fuels

After successful ignition, a WBT pot was placed immediately above the furnace body with 5 L of room-temperature water. The output was recorded for the flue analyzer (T-gas, O_2 , CO_2 , CO , NO , NO_x , SO_2 , SO_x , and hydrocarbons) and aerogel detector ($\text{PM}_{2.5}$) every 2 min. The ratio of the CO_2 and O_2 contents was calculated as the percentage of the inhaled smoke volume, and the current CO_2 concentration was calculated based on the relationship with the O_2 concentration which was equal to 13%.

As a result of the NO_x and SO_2 emissions in Fig. 5, the trend changes were quite different. NO and NO_x emission peaks were observed in the first 5 min, and a certain regularity was maintained before combustion began at 14 min. The order of NO and NO_x emission concentrations was $\text{WMP30} > \text{WMP15} > \text{WMP5}$. This trend was positively correlated with the nitrogen content of the derived fuel. The rigid PU used in the test had the highest nitrogen content of all samples, while the wood fuel pellets made from cedar had the lowest nitrogen content. As the nitrogen content of the reference mixture increased, the elemental analysis results showed the same increasing trend. NO_x concentrations of the WMP5 and WP samples showed little difference. The emission concentration of WMP30 decreased after 6 min of the combustion process. Carbon monoxide also exhibited the same trend. SO_2 emissions were detected in the initial combustion stage. As combustion progressed, the SO_2 emission concentration gradually decreased to the detection limit, so SO_2 could not be detected during the subsequent combustion process. Changes in the oxygen concentration of the exhaust flue gas were more consistent. The oxygen concentration reached a nadir 4 min after combustion began. As combustion progressed to the end, the oxygen concentration continued to rise slowly and finally almost approached the atmospheric oxygen concentration. This result indicated that the fastest oxygen

consumption in the furnace occurred at the beginning of combustion. The violent combustion reaction produced a large amount of emissions of CO, CO₂, and NO_x in a short period of time, and also released a large amount of heat energy.

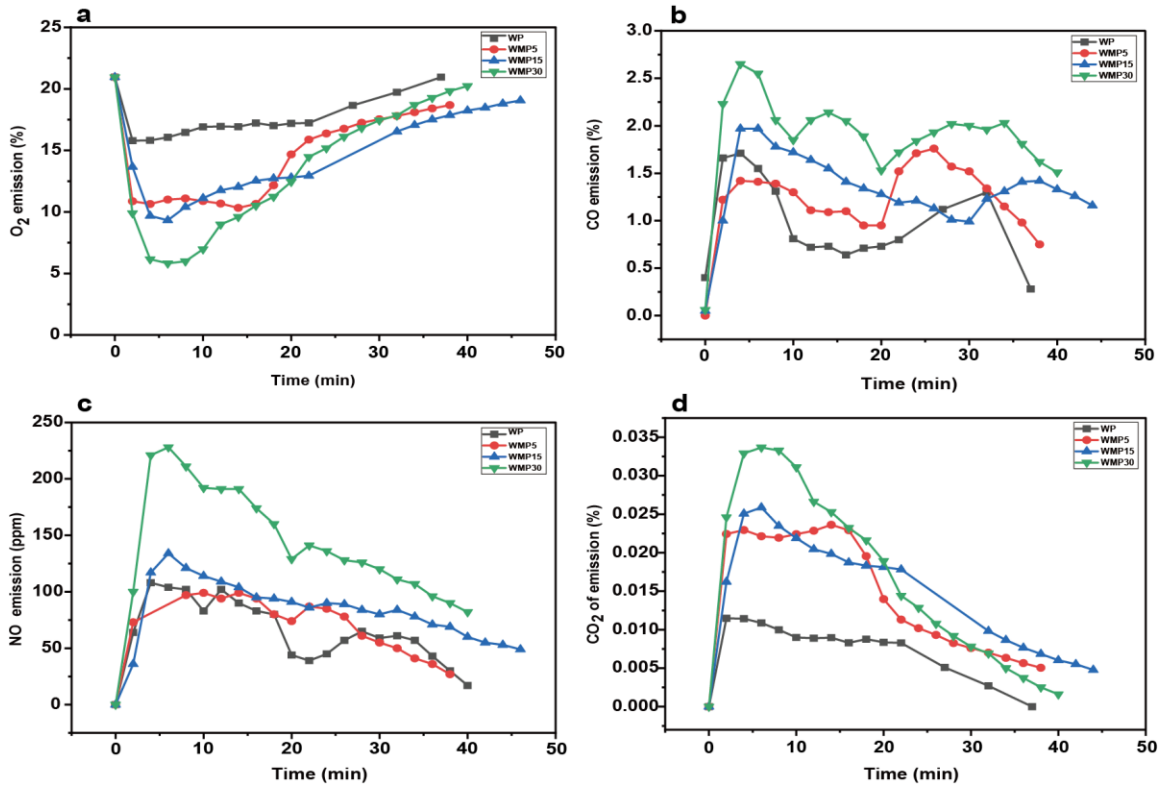


Fig. 5. Air pollution of waste refuse-derived fuel

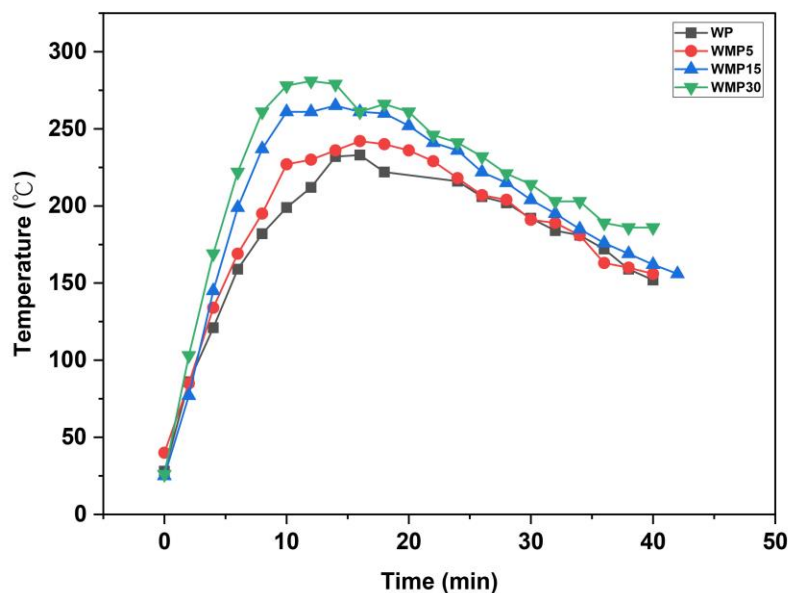


Fig. 6. Variations in the exhaust flue gas temperature during combustion of different refuse-derived fuel input pellets

As shown in Fig. 6, the exhaust gas temperature quickly rose, and the fuel in the furnace gradually burned as combustion progressed. The oxygen concentration in the furnace continued to rise to close to the atmospheric concentration, and the flue gas emission concentration also continued to decrease. In the performance of PM_{2.5}, it was observed that PM_{2.5} emissions increased with an increase in the amount of PU added. Overall, emission concentrations were in the order of WMP30 > WMP15 > WMP5 > WP. When the combustion began, the PM_{2.5} emission of the sample reached a peak. There was a continuous downward trend thereafter, and these results are consistent with those of previous studies. The main PM production was in the initial stage of ignition and combustion, and emission concentrations continued to decline to the end of combustion.

CONCLUSIONS

1. The oxidation behaviors of wood mixed with waste rigid polyurethane foam-derived fuels were investigated. According to the data of this study, waste *Cryptomeria* with low calorific value was mixed with waste rigid polyurethane foam to become fuel particles, and its calorific value increased as the ratio increased.
2. According to the Friedman equation, average activation energies of the wood mixed with 5%, 15%, and 30% of waste rigid polyurethane foam pellets were 175.7, 165.4, and 153.0 kJ·mol⁻¹, respectively.
3. The fastest oxygen consumption in the furnace occurred at the beginning of combustion. The violent combustion reaction produced a large amount of emissions of CO, CO₂, and NO_x in a short period of time, and also released a large amount of heat energy.
4. Waste *Cryptomeria* mixed with waste rigid polyurethane foam-derived fuels may be suitable for use as an alternative renewable energy fuel. It is necessary to strengthen the prevention and control of gas pollution emissions.

ACKNOWLEDGMENTS

This research was supported by grants from Taiwan Forestry Research Institute, the Council of Agriculture, Taiwan.

REFERENCES CITED

- Bilgili, F., Koçak, E., Bulut, Ü., and Kuşkaya, S. (2017). "Can biomass energy be an efficient policy tool for sustainable development?," *Renewable and Sustainable Energy Reviews* 71, 830-845. DOI: 10.1016/j.rser.2016.12.109
- Branca, C., Di Blasi, C., Casu, A., Morone, V., and Costa, C. (2003). "Reaction kinetics and morphological changes of a rigid polyurethane foam during combustion," *Thermochimica Acta* 399(1-2), 127-137. DOI: 10.1016/S0040-6031(02)00455-0
- Chen, W. H., Lu, K. M., Lee, W. J., Liu, S. H., and Lin, T. C. (2014). "Non-oxidative and oxidative torrefaction characterization and SEM observations of fibrous and ligneous

- biomass,” *Applied Energy* 114, 104-113. DOI: 10.1016/j.apenergy.2013.09.045
- Chen, Y., Shen, G., Su, S., Du, W., Huangfu, Y., Liu, G., Wang, X., Xing, B., Smith, K. R., and Tao, S. (2016). “Efficiencies and pollutant emissions from forced-draft biomass-pellet semi-gasifier stoves: Comparison of International and Chinese water boiling test protocols,” *Energy for Sustainable Development* 32, 22-30. DOI: 10.1016/j.esd.2016.02.008
- CNS 452 (2013). “Wood – Determination of moisture content for physical and mechanical tests,” Chinese National Standards, Taipei, Taiwan.
- CNS4713 (2005). “Method of test for ethanol-toluene extractives in wood,” Chinese National Standards, Taipei, Taiwan.
- CNS3084 (2004). “Method of test for ash in wood,” Chinese National Standards, Taipei, Taiwan.
- CNS 3085 (2004). “Method of test for holocellulose in wood,” Chinese National Standards, Taipei, Taiwan.
- CNS 14907 (2005). “Method of test for acid-insoluble lignin in wood,” Chinese National Standards, Taipei, Taiwan.
- CNS12108 (1987). “Method of test for acid-soluble lignin in wood and pulp,” Chinese National Standards, Taipei, Taiwan.
- CNS 10821 (1984). “Method for determination of inherent moisture of coal and coke,” Chinese National Standards, Taipei, Taiwan.
- CNS 10822 (1984). “Method for determination of ash of coal and coke,” Chinese National Standards, Taipei, Taiwan.
- CNS 10823 (1984). “Method for determination of volatile matter of coal and coke,” Chinese National Standards, Taipei, Taiwan.
- CNS 10824 (1984). “Method for calculation of fixed carbon of coal and coke,” Chinese National Standards, Taipei, Taiwan.
- Datta, J., and Włoch, M. (2017). “Recycling of polyurethanes,” *Polyurethane Polymers* pp. 323-358. DOI: 10.1016/B978-0-12-804039-3.00014-2
- Deng, Y., Dewil, R., Appels, L., Ansart, R., Baeyens, J., and Kang, Q. (2021). “Reviewing the thermo-chemical recycling of waste polyurethane foam,” *Journal of Environmental Management* 278, 111527. DOI: 10.1016/j.jenvman.2020.111527
- Friedman, H. L. (1964). “Kinetics of thermal degradation of char-forming plastics from thermogravimetry. Application to a phenolic plastic,” *Journal of Polymer Science Part C: Polymer Symposia* 6(1), 183-195. DOI: 10.1002/polc.5070060121
- Gama, N. V., Ferreira, A., and Barros-Timmons, A. (2018). “Polyurethane foams: Past, present, and future,” *Materials* 11(10), 1841. DOI: 10.3390/ma11101841
- Garrido, M. A., and Font, R. (2015). “Pyrolysis and combustion study of flexible polyurethane foam,” *Journal of Analytical and Applied Pyrolysis* 113, 202-215. DOI: 10.1016/j.jaap.2014.12.017
- Kissinger, H. E. (1956). “Variation of peak temperature with heating rate in differential thermal analysis,” *Journal of Research of the National Bureau of Standards* 57(4), 217-221.
- Kissinger, H. E. (1957). “Reaction kinetics in differential thermal analysis,” *Analytical Chemistry* 29(11), 1702-1706. DOI: 10.1021/ac60131a045
- Lin, L. D., Tsai, M. J., Chang, F. C., Ko, C. H., and Yang, B. Y. (2022). “Influence of torrefaction on the heating values and energy densities of hardwood and softwood,” *BioResources* 17(1), 316-328. DOI: 10.15376/biores17.1.316-328
- Lu, K. M., Lee, W. J., Chen, W. H., and Lin, T. C. (2013). “Thermogravimetric analysis

- and kinetics of co-pyrolysis of raw/torrefied wood and coal blends,” *Applied Energy* 105, 57-65. DOI: 10.1016/j.apenergy.2012.12.050
- Lu, S. Y., and Cho, C. L. (2014). “Effects of heat treatment on the chemical properties of three domestic plantation wood species,” *Forest Products and Industry* 33, 13-26.
- Luo, H., Bao, L. W., Kong, L. Z., and Sun, Y. H. (2018). “Revealing low temperature microwave-assisted pyrolysis kinetic behaviors and dielectric properties of biomass components,” *AIChE Journal* 64(6), 2124-2134. DOI: 10.1002/aic.16073
- NIEA R409.21C (2004). “Content determination method of carbon, hydrogen, sulfur, oxide and nitrogen in the waste-elemental analyzer,” Environmental Protection Administration, Taipei, Taiwan.
- NIEA R214.01C (2005). “The method to measure the heat value of the waste—Bomb calorimeter method,” Environmental Protection Administration, Taipei, Taiwan.
- Okoroigwe, E. C., Enibe, S. O., and Onyegebu, S. O. (2016). “Determination of oxidation characteristics and decomposition kinetics of some Nigerian biomass,” *Journal of Energy in Southern Africa* 27(3), 39-49.
- Ozawa, T. (1965). “A new method of analyzing thermogravimetric data,” *Bulletin of the Chemical Society of Japan* 38(11), 1881-1886. DOI: 10.1246/bcsj.38.1881
- Ozawa, T. (1971). “Kinetics of non-isothermal crystallization,” *Polymer* 12(3), 150-158. DOI: 10.1016/0032-3861(71)90041-3
- Park, J., Jung, I., Lee, K., Kim, M., Hwang, J., and Choi, W. (2018). “Case study in Korea of manufacturing SRF for polyurethanes recycling in e-wastes,” *Journal of Material Cycles and Waste Management* 20(4), 1950-1960. DOI: 10.1007/s10163-018-0718-5
- Rabemanolontsoa, H., and Saka, S. (2013). “Comparative study on chemical composition of various biomass species,” *RSC Advances* 3(12), 3946-3956. DOI: 10.1039/C3RA22958K
- REN21, R. (2018). *Global Status Report*, REN21 Secretariat.
- Sadhukhan, A. K., Gupta, P., and Saha, R. K. (2011). “Modeling and experimental studies on single particle coal devolatilization and residual char combustion in fluidized bed,” *Fuel* 90(6), 2132-2141. DOI: 10.1016/j.fuel.2011.02.009
- Singh, R., Krishna, B. B., Mishra, G., Kumar, J., and Bhaskar, T. (2016). “Strategies for selection of thermo-chemical processes for the valorisation of biomass,” *Renewable Energy* 98, 226-237. DOI: 10.1016/j.renene.2016.03.023
- Taiwan Environmental Protection Agency (2020). *Yearbook of Environmental Protection Statistics*, Environmental Protection Agency of Taiwan.
- Vanapalli, K. R., Bhattacharya, J., Samal, B., Chandra, S., Medha, I., and Dubey, B. K. (2021). “Inhibitory and synergistic effects on thermal behaviour and char characteristics during the co-pyrolysis of biomass and single-use plastics,” *Energy* 235, 121369. DOI: 10.1016/j.energy.2021.121369
- Xue, Y., Zhou, S., Brown, R. C., Kelkar, A., and Bai, X. (2015). “Fast pyrolysis of biomass and waste plastic in a fluidized bed reactor,” *Fuel* 156, 40-46. DOI: 10.1016/j.fuel.2015.04.033
- Yang, J., Rizkiana, J., Widayatno, W. B., Karnjanakom, S., Kaewpanha, M., Hao, X., Abudula, A., and Guan, G. (2016). “Fast co-pyrolysis of low density polyethylene and biomass residue for oil production,” *Energy Conversion and Management* 120, 422-429. DOI: 10.1016/j.enconman.2016.05.008

- Younis, M., Alnouri, S. Y., Abu Tarboush, B. J., and Ahmad, M. N. (2018). “Renewable biofuel production from biomass: A review for biomass pelletization, characterization, and thermal conversion techniques,” *International Journal of Green Energy* 15(13), 837-863. DOI: 10.1080/15435075.2018.1529581
- Zhang, X., Lei, H., Chen, S., and Wu, J. (2016). “Catalytic co-pyrolysis of lignocellulosic biomass with polymers: A critical review,” *Green Chemistry* 18(15), 4145-4169. DOI: 10.1039/C6GC00911E

Article submitted: April 25, 2022; Peer review completed: July 11, 2022; Revised version received and accepted: October 25, 2022; Published: November 30, 2022.
DOI: 10.15376/biores.18.1.778-791